



Extreme lightweight structures: avian feathers and bones

Tarah N. Sullivan¹, Bin Wang², Horacio D. Espinosa³ and Marc A. Meyers^{1,*}

¹ University of California, San Diego, La Jolla, CA, USA

² Shenzhen Institute of Advanced Technology, Chinese Academy of Sciences, Shenzhen, People's Republic of China

³ Northwestern University, Evanston, IL, USA

Flight is not the exclusive domain of birds; mammals (bats), insects, and some fish have independently developed this ability by the process of convergent evolution. Birds, however, greatly outperform other flying animals in efficiency and duration; for example the common swift (*Apus apus*) has recently been reported to regularly fly for periods of 10 months during migration. Birds owe this extraordinary capability to feathers and bones, which are extreme lightweight biological materials. They achieve this crucial function through their efficient design spanning multiple length scales. Both feathers and bones have unusual combinations of structural features organized hierarchically from nano- to macroscale and enable a balance between lightweight and bending/torsional stiffness and strength. The complementary features between the avian bone and feather are reviewed here, for the first time, and provide insights into nature's approach at creating structures optimized for flight. We reveal a novel aspect of the feather vane, showing that its barbule spacing is consistently within the range 8–16 μm for birds of hugely different masses such as Anna's Hummingbird (*Calypte anna*) (4 g) and the Andean Condor (*Vultur gryphus*) (11,000 g). Features of the feather and bone are examined using the structure-property relationships that define Materials Science. We elucidate the role of aerodynamic loading on observed reinforced macrostructural features and efficiently tailored shapes adapted for specialized applications, as well as composite material utilization. These unique features will inspire synthetic structures with maximized performance/weight for potential use in future transportation systems.

Introduction

Through tens of millions of years of evolution [1] birds have developed to contend with the challenges of flight, a highly complex mode of locomotion that man only came to grasp about one hundred years ago. The bird's designs includes a toothless keratinous beak [2] filled with cancellous bone [3], wing stroke efficiency [4], fusion of parts of the skeleton [5], and strong yet lightweight feathers and bones. Bird flight is believed to have evolved by dinosaurs jumping to catch their prey, providing an evolutionary advantage with wings that captured air [6]. This jumping led to gliding, and eventually flapping flight.

Background

Arguably the most crucial evolutionary feat to allow for bird flight, the wing is a system in which the skeleton and feathers act together to allow for a high lift-to-weight ratio. The wing skeleton is particularly lightweight; unlike terrestrial vertebrates' marrow-filled bones, most bird wings are composed of hollow bones, similar to the bones of bats and pterosaurs [7]. These hollow (pneumatic) bones connect to the pulmonary system and allow air circulation which increases skeletal buoyancy [8–10]. The remiges, or flight feathers on the wings of birds, consist of a main shaft (rachis and calamus) and an interlocking feather vane composed of barbs that branch from the rachis and barbules that branch from barbs (Fig. 1). Neighboring barbules adhere to one

*Corresponding author. Meyers, M.A. (mameyers@ucsd.edu)

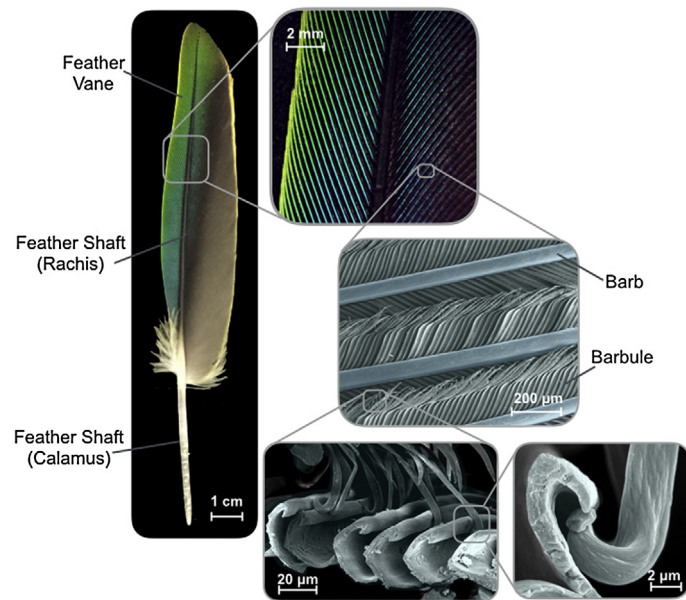


FIGURE 1

The flight feather is composed of the feather shaft (rachis and calamus) and the feather vane (barbs and barbules). Barbs are foam-filled asymmetrical beams that branch from the rachis and barbules are minute hooked beams and grooves that branch from barbs to interlock with each other. The two bottom SEM images are taken from T.N. Sullivan et al. (2016) [108].

another via hook-and-groove structures to form a cohesive feather vane. This complex design of the modern feather evolved in the Late Jurassic period with the advancement of flight [1]. An example of a precursor to the modern feather, thought to have belonged to a non-avian dinosaur ~99 million years ago, was recently discovered preserved in Burmese amber (Fig. 4c) [11]. It lacks several features of the modern feather including the interlocking barbule connections and a fully developed rachis. The modern vane is an ingenious structure that is not sealed, but contains channels between barbules through which air can flow [12,13].

Birds have been very successful in populating Earth, with nearly 10,000 recognized species constituting an extremely diverse class of animals [14]. While all birds have certain coinciding bone and feather features, to better understand their efficiency it is critical to note the aspects that differ between them due to distinct environmental constraints. First, birds range enormously in size from hummingbirds that are about 2 g with a wingspan of 8 cm, to the 11 kg Andean condor with a wingspan greater than 3 m [14,15]. Besides sheer differences in size, birds differ in flight style. Some birds achieve flight through flapping their wings and soaring (i.e. vultures, eagles); others through flapping and gliding (i.e. seagulls, pelicans) [16,17]. Additionally, certain birds mainly flap their wings (i.e. ravens, ducks, pigeons, crows), a few birds hover (i.e. hummingbirds), and lastly some are flightless (i.e. ostriches, peacocks) [18]. Moreover, some birds dive and swim (i.e. ducks, auks), while others do not. Each of these types of birds have slightly different environmental constraints on their physiology, which result in specific variations to their bone and feather structure.

In most birds the skeleton extends only half-way from the shoulder to the wing tip and therefore the majority of the area of the wing is supported by flight feathers [19]. Wing flight feathers

include primaries that branch from the hand skeleton and secondaries that attach to the edge of the ulna. Flight feathers are anchored by a reinforced follicle which transfers the bending and torsional moments from the base of the feather to the skeleton [7]. Primaries do not have any freedom of movement relative to the bones to which they are rigidly attached. Secondaries, on the other hand, are able to hinge up and down relative to the ulna through flexible attachment. When the elbow and wrist joints are fully extended, primaries spread out and secondaries are pulled downward by the tightening of the postpatagial tendon, which results in an increase in camber of the wing [7]. In flapping flight, the elbow and wrist joints are flexed, resulting in a reduced wingspan and loosening of the tendon, providing a less cambered wing shape. Through this system, individual feathers allow for wing adaptability, while transferring the bulk of loading to the more robust skeleton of the bird. Together, the wing skeleton and feathers form an organic airfoil capable of handling the intense loads of flight. Here we review the structure, mechanics, and composition of the avian feather and bone to understand how they maintain integrity with a minimum weight penalty. While the material composition of the feather and avian bone is the same across species, they have different design adaptations for specific environments. The commonalities in the design principles of the avian bone and feather are discussed to gain insight into the application of these concepts to engineered structures and materials.

Wing loading in flight

Since the main focus of this paper is to investigate the extreme lightweight structures of bird wings, and not the aerodynamics of flight, loading is simplified to static forces. In flight a lift force acts upwards, resulting in a bending moment about the wing's connection to the body (Fig. 2a). Each wing is loaded with a force = $kmg/2$, where mg is the weight of the bird, and k is a parameter that represents the load multiplication factor. For steady loading and for gliding, $k = 1$; for flapping, landing and takeoff, $k > 1$.

The wing can be considered as a series of thin airfoils for which the aerodynamic center of lift occurs at 25% of the chord length from the leading edge of the airfoil [20]. These points of lift are represented by the solid dots in Fig. 2b. If the force of each point of lift is represented as F_i , these can be related to the force on the entire wing by:

$$\sum_{i=1}^n F_i = \frac{kmg}{2}. \quad (1)$$

While the entire wing skeletal systems of pterosaurs and bats are modified to form structures that resist bending and torsion, only the inner wing skeleton of the bird has this function as flight feathers maintain this distally [7,21]. Because the ulna is roughly perpendicular to the humerus in flight and cannot rotate up and down relative to it, bending moments applied to the outer wing become torsional moments when loads are transferred to the humerus [7] (Fig. 2b). Additionally, since most of the area of the wing is behind the radius and ulna, there is a torsional moment applied to the humerus from the secondary flight feathers. In Fig. 2b the bending and torsion axes are drawn for the humerus. The locations of the points of lift are each represented as O_i , where the torsion moment arm is AO_i and the bending moment arm is BO_i . Torsional (T) and bending (B) loads on the humerus for the

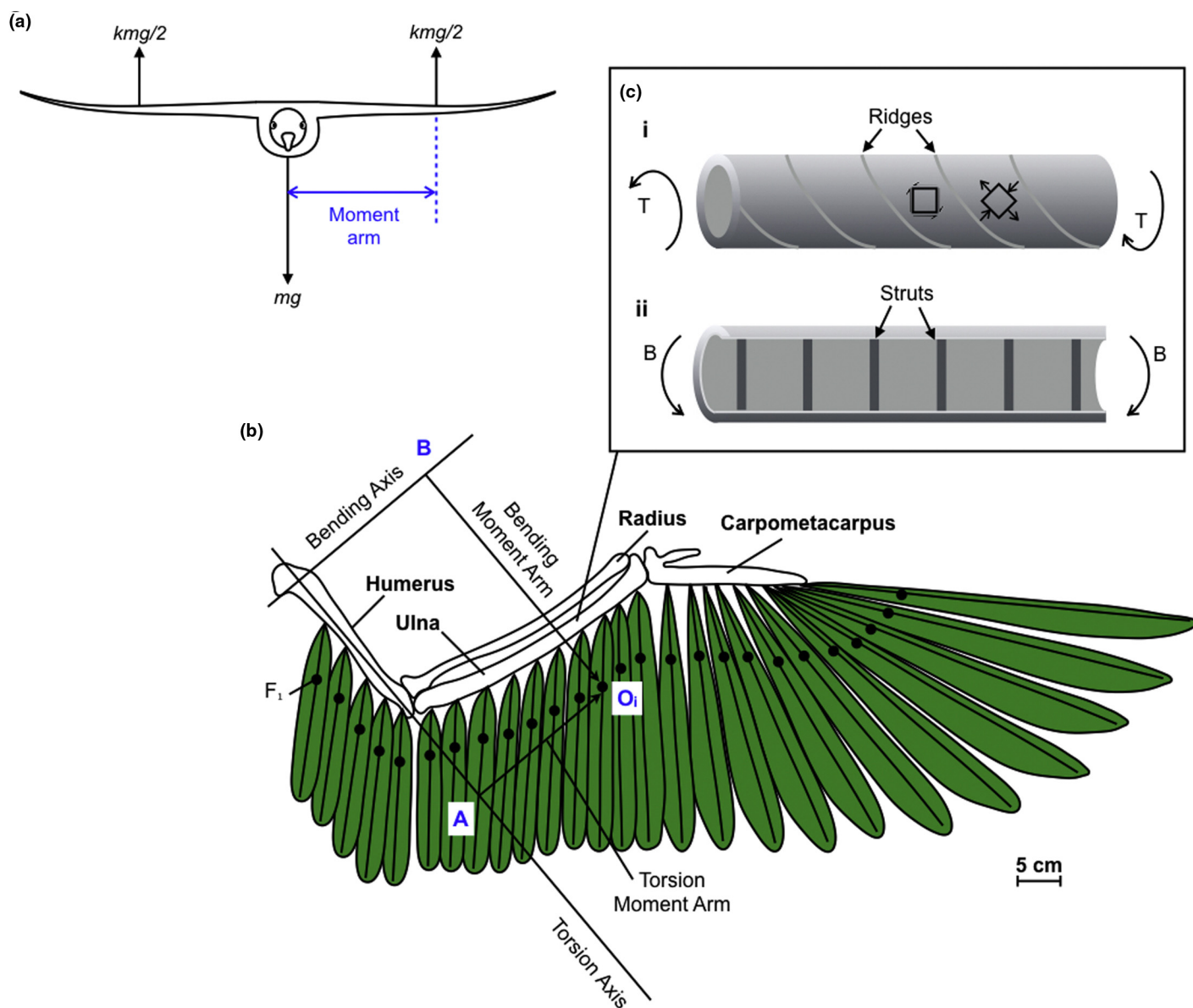


FIGURE 2

(a) The upward in-flight lift forces result in a bending moment about the wings connection to the body. When the bird is gliding $k = 1$; however in take off, landing or flapping, $k > 1$. (b) The skeletal system and flight feathers of the bird wing. The wing skeleton is a modified quadruped arm skeleton with a *humerus* (attached to the main flight muscles), *ulna*, *radius* and *carpometacarpus* (a fusion of the wrist and knuckles). The solid dots mark the centers of lift for each feather. The force of each of these points is represented as F_i and the location as O_i . Bending moments occur in the radio-ulna and are transmitted through the elbow joint as a torsional moment. The torsion and bending axes are drawn for the humerus, where B represents the bending axis and A the torsional axis. Adapted from C. Pennycuick (1967) [19]. (c, i) Schematic diagram of how the ridges in avian bone may form as a result of torsional forces (T). These ridges are aligned with the direction of maximum tensile force indicating that ridges increase resistance to tensile failure. (c, ii) Simplified diagram of internal struts strengthening the bending stiffness of avian bone.

entire wing can therefore be represented as:

$$T = \sum_{i=1}^n F_i A O_i; \tag{2}$$

$$B = \sum_{i=1}^n F_i B O_i; \tag{3}$$

For the ulna, the same procedure can be repeated.

Bending and torsion

Basic Mechanics equations connect the applied forces to internal stresses in bones and feathers, and those in turn dictate the

architecture and design of the structure. Bones and feathers are subjected to bending stresses that are defined by [22]:

$$\sigma = \frac{Mc}{I}. \tag{4}$$

where $M = Fd$, in which F is the magnitude of the applied force and d is the moment arm; c is the distance from the neutral axis to the object's surface, and I is the area moment of inertia.

Likewise in torsion, the maximum shear stress is expressed as [22]:

$$\tau = \frac{Tc}{J}. \tag{5}$$

where T is torque, c is the radius of the section, and J is the polar moment of inertia.

The maximum values of I and J , for a specific weight per unit length, minimize the normal and shear stresses of bones and feathers. The feather and bone can be modeled as a hollow cylinder, a section that provides a balance between bending and torsion resistance. For a hollow cylinder [23]:

$$I = \frac{\pi(R_0^4 - R_i^4)}{4}; \quad (6)$$

$$J = \frac{\pi(R_0^4 - R_i^4)}{2}. \quad (7)$$

where R_0 denotes the outer radius, and R_i is the inner radius. While thick walls allow for a higher value of both I and J they result in a heavy structure. Thin walls, however, eventually lead to buckling, an undesirable result. To overcome this, nature provides two ingenious solutions: internal struts that oppose ovalization and retard buckling in bending (Fig. 2c); and internal foam resulting in the strengthening of the walls. The former occurs in avian bone, and the latter in the feather.

Thin, dense exterior with reinforcing internal structures

Thin, dense exterior

Since both the wing bones and feathers of birds are subject to bending and torsion, it is expected that they have several overlapping structural features. One of these characteristics is a thin, dense exterior with a hollow or less compact interior. This design allows for lightweight resistance to these external loadings. In bending, the stiffness is given by the product of the area moment of inertia and the material's Young's modulus. Therefore material positioned further from the neutral axis is more effective in resisting bending because it undergoes more extension and compression than material close to the neutral axis [24]. In torsion, thin-walled closed cross-sections offer a high torsional stiffness, which is given by the product of the area enclosed by the thin wall and the material's shear modulus. Hence for combined loading, a thin-walled closed cross-section offers optimal performance in both bending and torsion. The other variable contributing to structural stiffness is the material modulus, which increases with density [25,26]. Therefore, structures with a dense exterior wall are expected in both avian bones and feathers. Moreover, modulation of density and wall thickness is expected to depend on wing location because of spatial variations in bending and torsional moments.

As previously stated, many birds have some hollow (pneumatic) bones; across 24 species 70% of bird humeri and 30% of femori were found to be pneumatic [27]. Fig. 3 shows micro computerized-tomography cross sections of the wing bones of the (a) Wandering Albatross (*Diomedea exulans*), (b) Turkey Vulture (*Cathartes aura*), and (c) California Condor (*Gymnogyps californianus*). These wing bones exhibit similar features between the three species: a hollow, circular mid-cross section with struts, ridges and webbing occurring toward the ends of each bone. Pneumatic bones are thinner walled [28] and more dense [25] than marrow-filled bones and have a flexural modulus of 6.9–7.7 GPa [27]. In comparison with various animals, birds have the most dense bone ($\sim 2.15 \text{ g/cm}^3$), which increases their stiffness and strength, followed closely by the bat ($\sim 2.0 \text{ g/cm}^3$), another flying vertebrate,

with rodents trailing behind ($\sim 1.85 \text{ g/cm}^3$) [25]. This is the density of the solid bone, which is composed of hydroxyapatite ($\rho = 3.14 \text{ g/cm}^3$), collagen ($\rho = 1.35 \text{ g/cm}^3$), and water ($\rho = 1 \text{ g/cm}^3$) [29].

Similarly, the feather shaft has a thin, compact exterior (cortex) with a hollow, circular base (calamus), which anchors the feather under the skin, and a foam-filled rectangular rachis (Fig. 4a,b). Although both components consist entirely of β -keratin, the rachis' medullary foam density ranges from 0.037 to 0.08 g/cm^3 , while the cortex density ranges from 0.66 to 0.81 g/cm^3 [30,31]. The cortex material is over 100 times stiffer than the medullary foam, which has an elastic modulus of 2.5–6.5 GPa [30–34], whereas the foam's modulus is 0.01–0.03 GPa [30,31]. Due to this large difference, the geometry of the cortex dominates the flexural stiffness of the shaft [30,32,35]. Adding complexity to the hierarchy, both bones and feathers are comprised of fibers which are directionally aligned in such a manner to maximize resistance to bending and torsion. In the bone, the collagen fibers form lamellae which are interspersed with hydroxyapatite crystals that are structured at the nanoscale. In feathers, the β -keratin fibers are aligned in different orientations to enhance the stability. These topics will be discussed later in this overview.

Reinforcing internal structures

Both the avian bone and feather have internal reinforcing structures that strengthen their design. Due to the high metabolic cost and increased weight of creating more bone or cortex material, it is speculated that these reinforcing structures develop within the wing bone and feather in response to specific stresses of flight.

Ridges

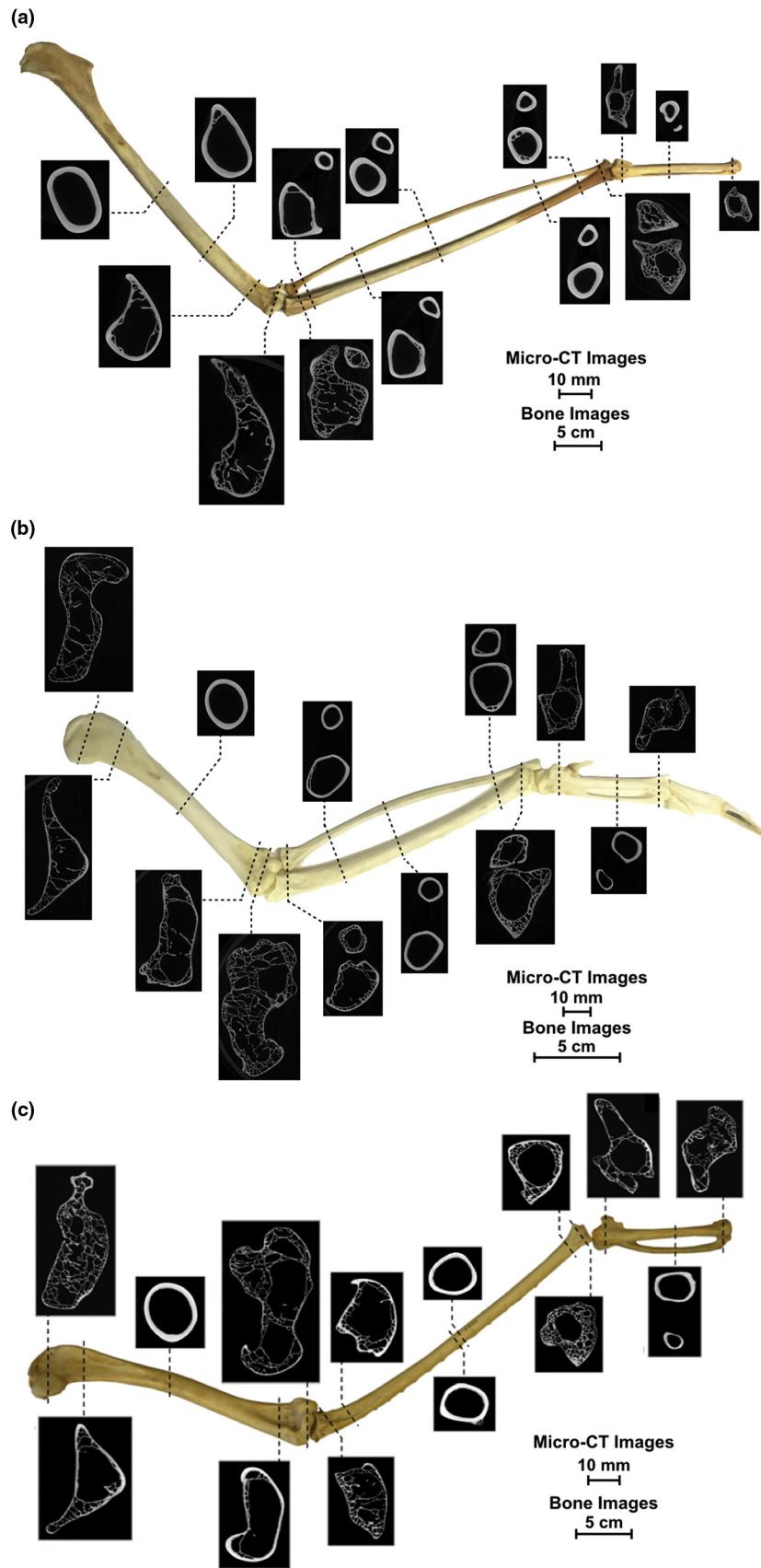
Ridges are protrusions of bone or cortex that lie flat against the interior walls of the bone or feather (Fig. 5a,c). In avian bone they generally develop at -45° to the horizontal axis of the bone, to increase the resistance of the structure to the large tensile stresses that develop in these directions in torsion [22]. Ridges along this angle are most effective because in torsion axial stresses occur at -45° to the longitudinal axis [36] (Fig. 2c).

In many flight feathers multiple cortex ridges run internally along the length of the rachis' dorsal surface, slowly becoming fewer and less sharply defined distally [32,35]. These small ridges stiffen feathers in dorso-ventral flexure, but do not strongly influence lateral movements [32]. Cortex ridges occur on the dorsal surface because the feather experiences the largest stress in compression during the bird's down stroke, occurring on the dorsal side of the feather shaft [37].

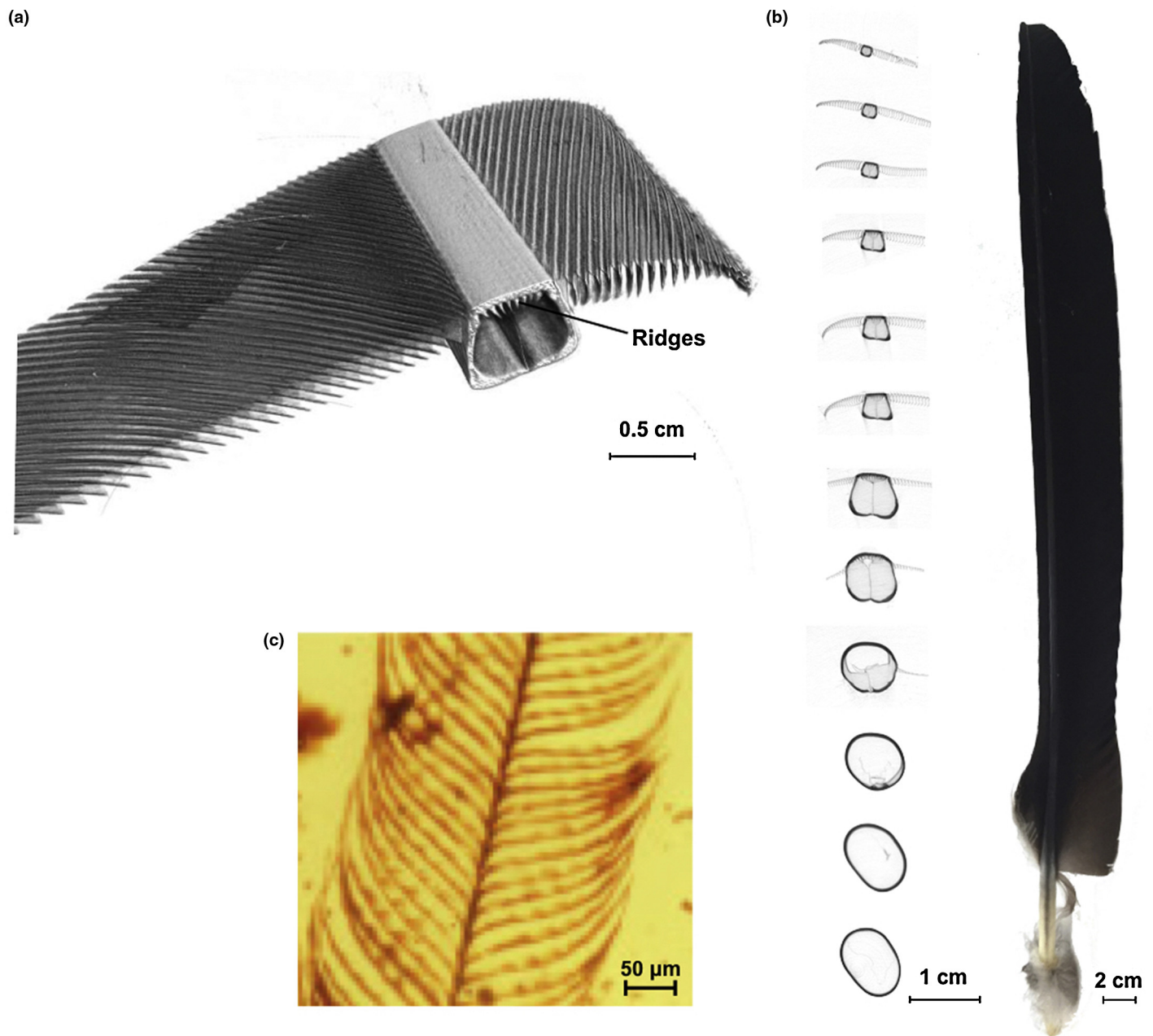
Struts and foam

Struts are isolated rods that stretch across the interior of pneumatic bone (Fig. 5b). They are mainly found on the ventral side of wing bones of flying birds, appearing to be at locations that have a higher risk of local buckling due to combined bending and torsion loading [7,8,17,36] (Fig. 2c).

Taking a different approach to resist local buckling, the feather does not have struts, but the majority of it (the rachis) is foam-filled (Fig. 5d). This fibrous internal medullary foam is considered closed-celled and provides 96% of the transverse compressive rigidity [31]. However, closer examination reveals that the cell

**FIGURE 3**

Micro computerized tomography scans of the wing bones of the: (a) Wandering albatross (*Diomedea exulans*), which has the largest wingspan of any living bird, (b) Turkey Vulture (*Cathartes aura*), and (c) California Condor (*Gymnogyps californianus*). The bones of all three species have hollow, circular mid-cross sections and reinforcing structures toward the ends of each bone. Fig. 3c from E. Novitskaya et al. (2017) [36].

**FIGURE 4**

Micro computerized tomography (μ -CT) generated images of an Andean Condor (*Vultur gryphus*) primary feather: (a) shows the feather vane and details of the ridges in the rachis while (b) demonstrates the shape change along the length of the feather shaft from circular to rectangular (part of image is from B. Wang et al. (2016) [52]). Precursors to modern feathers were much less developed as shown in (c) by the plumage of a non-avian dinosaur from \sim 99 million years ago preserved in Burmese amber (image from L. Xing et al. (2016) [11]).

walls are indeed porous and consist of fibers. The foam also absorbs the bulk of energy, providing a rachis with a strength higher than the sum of each of its components [31]. Similar to how the bird has evolved to have these unique internal reinforcement features, types of birds have adapted to their specific environment with more specialized structures.

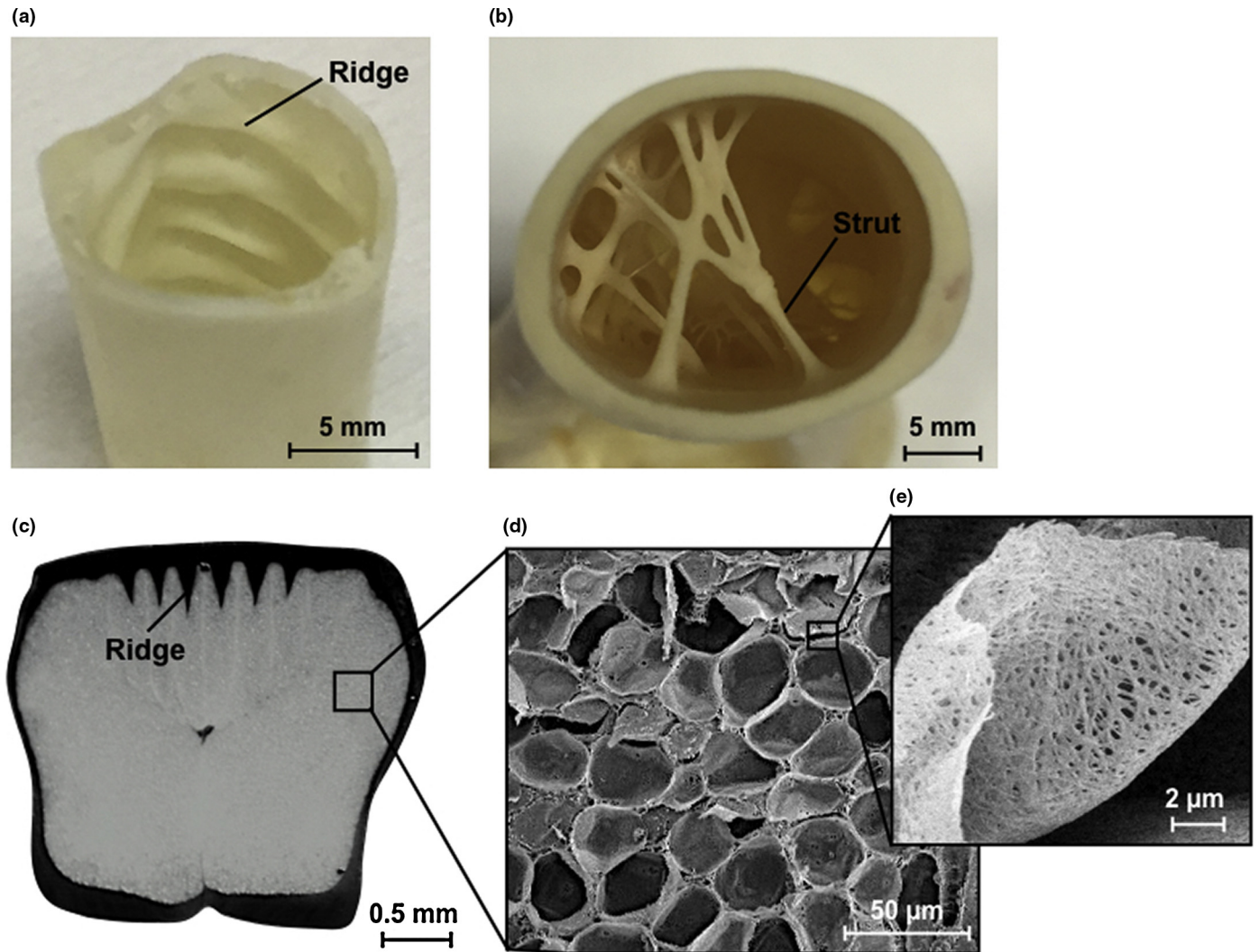
Efficiently tailored designs based on specific conditions

The effect of bird body mass on the wing bone and feather

Wing bone

Since the body mass of birds differs so greatly, their skeletal structure has evolved to meet different requirements of loading,

and certain trends have been discovered as body mass rises. First, the length of wing bones increases faster with body mass than the length of hind limb bones of birds; however the trend is reversed for the diameter of the bones, with hind limb bone diameters increasing faster than wing bone diameters [38]. This trend reflects the significance of creating longer airfoils (through increasing the length of wing bones) to support a heavier load. Additionally, the bending strength and flexural Young's modulus of the pneumatic bones of birds was found to negatively correlate with body mass [27]. Perhaps this reflects a materials limit in pneumatic bone forcing feathers to sustain more of the loading for more massive birds.

**FIGURE 5**

Internal reinforcements in the avian bone and feather: (a) ridges in the ulna of the Turkey Vulture (*Cathartes aura*), (b) struts toward the distal end of a Cape Vulture (*Gyps coprotheres*) humerus bone, (c) ridges in the American White Pelican (*Pelecanus erythrorhynchos*) feather, (d) medullary foam of the feather; (e) foam wall exhibiting porosity, thus forming a “foam-in-a-foam”.

Flight feather

Since flight feathers are necessary for bird flight [39], it is presumed that an increase in body mass would have an effect on them. In order for a more massive bird or flying object to maintain lift, it must increase its cruising airspeed or its wing size [40]. The increase in the size of feathers, L , with mass, m , can be expressed as a first approximation, assuming geometrical scaling. The length L and width W are hypothesized to be related to the mass m by: $L \propto m^{1/3}$, and $W \propto m^{1/3}$. This 1/3 slope represents a self-similar geometric relationship assuming a spherical body whose radius increases with the volume to the power 1/3. Fig. 6a–c compares the experimental slope for feather length (0.30–0.34) [41,42] mid-shaft width (0.32–0.37) [41–43], and barb length on the trailing (0.27) and leading (0.25) [41] edge of the vane with the ideal 1/3 mass dependence. This trend demonstrates a quantifiable scaling relationship between the mass of birds and wing size. Interestingly, we found that the spacing between hooked, trailing barbules remains within a range of 8–16 micrometers, with no apparent dependence on the mass of bird (Fig. 6d).

The gap between barbules (Fig. 7a) includes a thin membranous flap extending from each barbule to cover the space in between barbules so that the vane is able to capture more air. This is thought to allow the vane to act as an assembly of one-way valves [12]. During the upstroke (recovery stroke) the bird’s primary feathers separate to allow air-flow through and prevent excessive downward forces on the wing [44]. We propose that these barbule flaps assist in preventing unwanted forces in the upstroke by allowing air to flow through the feather dorsally. In the downstroke (power stroke), however, the flaps do not allow air through and therefore maximize the capture of air by the feather. The simplified additively manufactured model of the flap structure within the feather vane is shown in Fig. 7b–d to demonstrate this. Thin, flexible flaps branch from hooked and grooved barbules to cover spaces between them. When air is blown at the bioinspired vane from the dorsal direction the flaps open (Fig. 7c) (where circles denote the location of airflow); however, when air is blown ventrally the flaps remain closed (Fig. 7d). Fig. 7e,f shows the similarity of barbule spacing, yet remarkable difference in feather

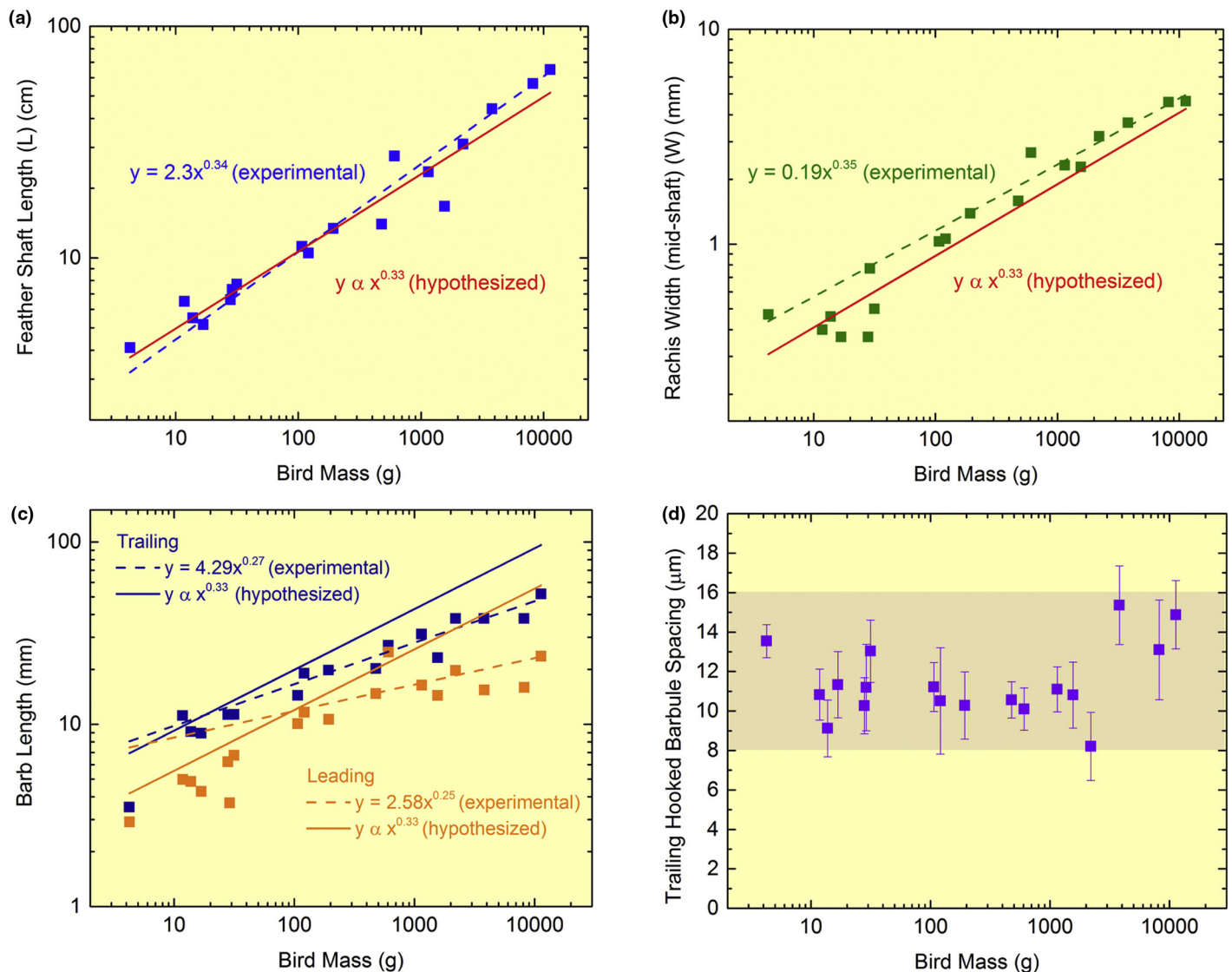


FIGURE 6 Scaling trends between the total bird mass and dimensions of the feather at different hierarchical levels [41]. The total feather shaft length scales with bird mass (a) following the trend $y = 2.3x^{0.34}$ with an R^2 value of 0.95 (where measurement uncertainty is ± 0.05 cm). Similarly, the width of the feather shaft at its midpoint scales with bird mass exponentially (b) following the trend $y = 0.19x^{0.35}$ with an R^2 value of 0.95 (measurement uncertainty is ± 0.02 mm). The barb length of the trailing and leading feather vane (c) follow $y = 4.29x^{0.27}$ ($R^2 = 0.91$), and $y = 2.58x^{0.25}$ ($R^2 = 0.83$) respectively (standard deviations range from 0.02 to 0.2 mm). For comparison $y \propto x^{1/3}$ is plotted in both (a), (b) and (c). Surprisingly, the spacing between trailing hooked barbules (d) does not follow this trend and ranges between 8 and 16 μm across all bird masses.

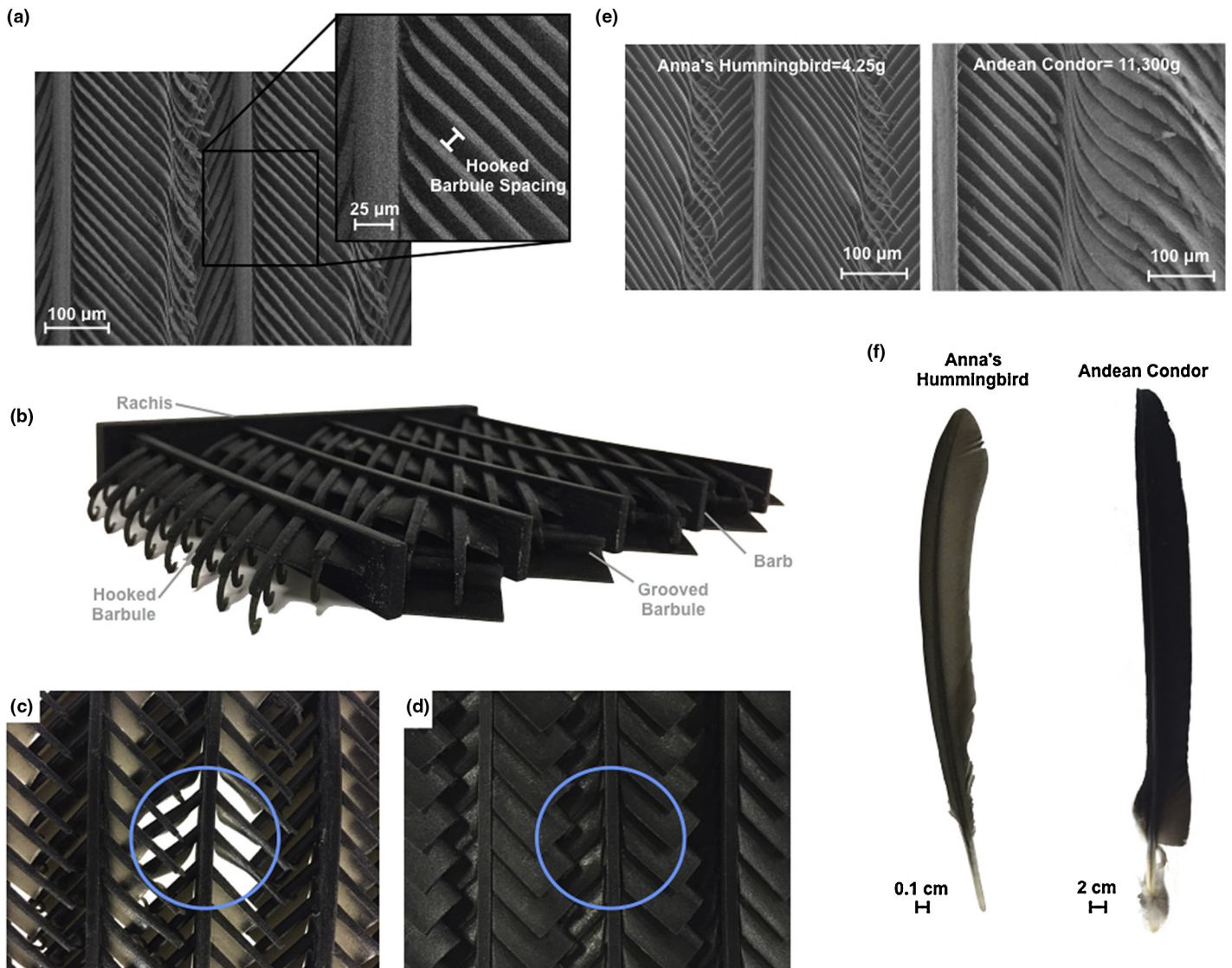
size between the Anna’s Hummingbird (*Calypte anna*) and the Andean Condor (*Vultur gryphus*). The reason for the constancy in barbule spacing (8–16 μm) is proposed to be to retain low permeability of air through the feather independent of bird size. The feather must balance air flow with maintenance of its interlocking structure.

Another interesting aspect of the flight feather is that its distal end is relatively more flexible (when normalized by mass) in larger birds than in smaller birds, as was demonstrated by Worcester [42] in a study involving 13 different species of birds ranging from 0.02 kg to 11 kg. One of the benefits of more flexible feathers in larger birds is the potential for higher lift generation; more flexible wings have demonstrated greater lift production in flapping flight [45] as well as in the flight of insects [46].

The effect of flight style and diving on the wing bones and feathers

Wing bones

As stated previously most birds have some pneumatic bones, the exceptions generally being birds that share the characteristic of diving [27,47]. It is thought that to maintain strength in impact and prevent excess buoyancy their bones are marrow-filled. Besides a lack of pneumatization, some diving birds dispossess certain macro- and microstructural torsional-resistant characteristics [47]. Torsion-resistant features found in the humerus of most birds include thin bone walls, a circular cross section, oblique collagen fibers, and laminar tissue arrangement [47]. The humeri of the aforementioned diving birds are oval-shaped and thick-walled; examples of variation in bone cross section are shown in

**FIGURE 7**

An example of the barbule spacing dimension is shown in (a). A bioinspired model created by additive manufacturing (b) was used to show the behavior of the barbule membrane flaps [41]. This model is shown with air blown dorsally (c) and ventrally (d) at the vane, where circles represent the location of airflow. The similarities between the micro-scale barbules of the Anna's Hummingbird (*Calypte anna*) (left) and the Andean Condor (*Vultur gryphus*) (right) are demonstrated in (e), while the macro-scale differences are shown in (f).

Fig. 8a,b. Furthermore, these birds have little lamellar tissue and mostly longitudinal collagen fibers, indicating that axial compression and tension are significant elements of bone loading for these cases [47]. As witnessed with diving birds, the optimum value of internal to external diameter varies based on the main function of the bone [28].

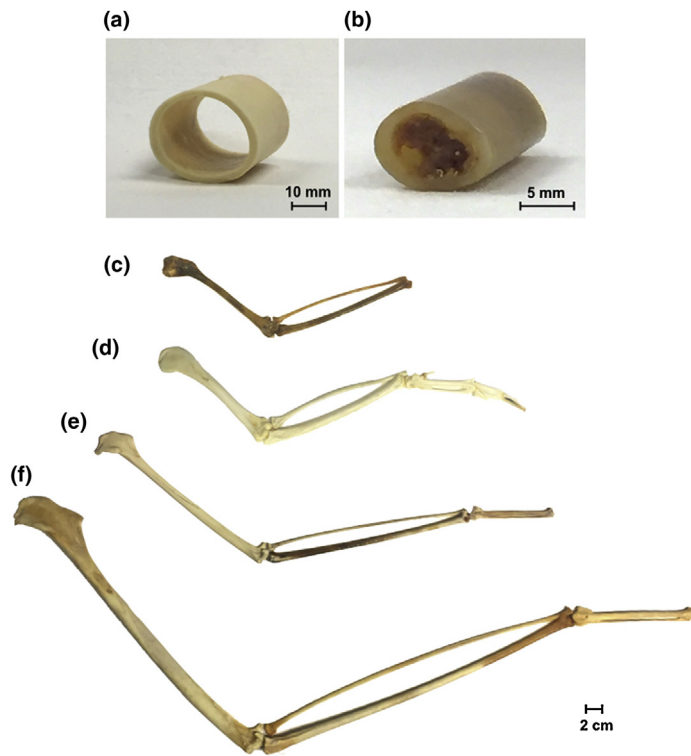
Since bones are in a constant state of growing and re-growing (remodeling) the reinforcing structures of struts and ridges form in an as-needed basis [48]. Struts and ridges, for example, were found in soaring and gliding birds, but not in flightless birds [7]. Additionally, the humerus of soaring and gliding birds is slightly more dense than the ulna to provide better support for the bird body and redistribute stresses [17].

The wing curvature, or distance between the center of the bone to the axis passing through the midpoints of the ends of the bone, determines the flight style of the bird [49]. Fig. 8c–f shows the wing skeletons of several birds. With increased curvature between the

radius and ulna, there is larger space for musculature in the forewing. Birds with a larger curvature between the radius and ulna are therefore more coordinated in unsteady flight [50]. As shown in Fig. 8e, the Laysan albatross is an example of a bird with minimal musculature within the forelimb. Because of this, it has uncoordinated takeoffs and landings; however it can dynamically soar for long periods of time due to its large wingspan.

Flight feathers

The general shape of the flight feather shaft transitions from round to rectangular at about 20% along the cross-sectional length of the feather shaft. The transition enables the tailoring of flexural and torsional stiffness subject to the constraint in wing thickness variations from the proximal to distal ends. Interestingly, this is strikingly different from the feathers of flightless birds (i.e. ostrich and peacock) which do not develop a strong rectangular shape throughout their entire length (Fig. 9a,b) [31,51,52]. The square

**FIGURE 8**

The mid-humerus of the Cape Vulture (*Gyps coprotheres*) (a) has high torsion resistance, while the mid-humerus of the California Gull (*Larus Californicus*) (b) has low torsional resistance. Wing bones of the (c) California gull (*Larus Californicus*), (d) Turkey Vulture (*Cathartes aura*), (e) Laysan albatross (*Phoebastria immutabilis*), (f) Wandering albatross (*Diomedea exulans*) have differing degrees of curvature between the radius and ulna.

shape of the flight feathers of flying birds is particularly efficient, since square tubes possess, for the same cross-sectional area and thickness, a higher stiffness per unit area than circular ones, and additionally resist ovalization during flexure [52]. This absence of ovalization enhances the flexural stiffness of the rectangular tube because the area moment of inertia does not decrease in flexure (as it does in ovalization). However, the rectangular shape makes the compressed dorsal region susceptible to local buckling, explaining the presence of internal ridges and the foam filling to compensate for this effect. These are shown in Fig. 5c and are also present in Fig. 9.

The rachises of birds exhibit various structural differences between species. In a comprehensive study comparing aspects of the barn owl and pigeon rachis it was found that the barn owl rachis has a higher area moment of inertia, yet fewer structurally rich features (such as dorsal ridges) when compared with the pigeon [32]. These two birds are of comparable body mass, though they differ in wing size and flight style. Fig. 9c further demonstrates that structural ridges are present in the feathers of certain birds, and absent from others. While structural features of the avian bone and feather are tailored to the flight or lifestyle of the bird, their material composition is the same across all species.

Hierarchical composite

Although the feather is composed solely of β -keratin, and avian bone consists primarily of collagen and hydroxyapatite, they can

both be considered composites at the micro- and nano-scales. This allows for material properties to vary throughout their respective lengths to conform to necessary loading requirements.

Avian bone: from nanostructure to mesostructure

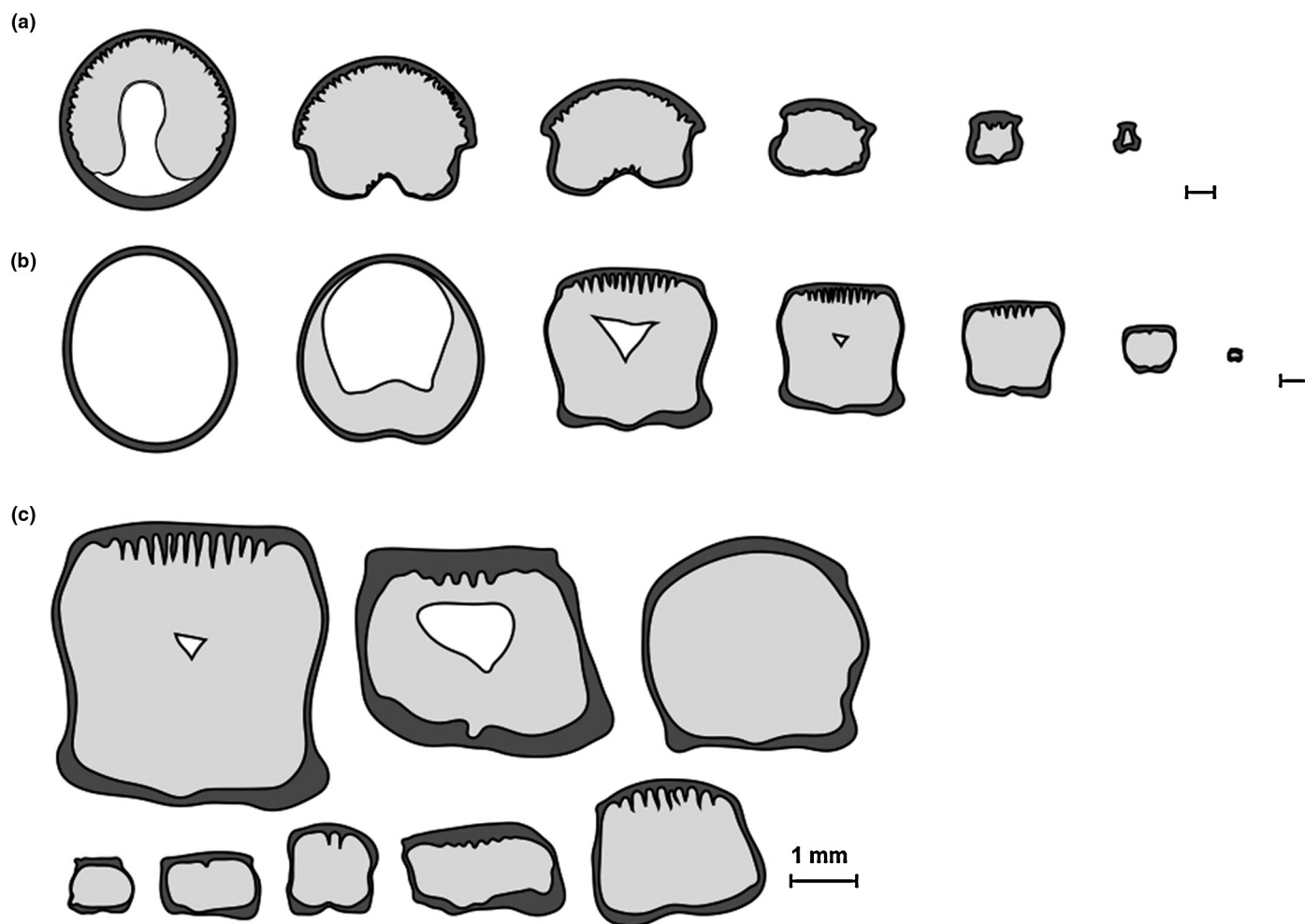
Bone is composed of several levels of hierarchical organization (Fig. 10a): (1) the sub-nanostructure (below a few hundred nanometers): tropocollagen molecules, mineral crystals, non-collagenous proteins; (2) the nanostructure (hundreds of nanometers–1 μm): collagen fiber bundles, collagen fibrils; (3) the sub-microstructure (1–10 μm): lamellae of cortical bone that surround osteon; (4) the microstructure (10–500 μm): Haversian systems, osteons; (5) the macrostructure: cancellous (spongy interior) and cortical bone (dense “outer shell” of bone) [53–59]. This level of organization allows for the material properties of bone to vary throughout the structure. In the avian humerus, for example, hardness was found to vary along the length, being the greatest in the center of the bone [60]. This may be due to adaptive remodeling of bone in response to the stresses of flight, or because the bone’s mid-shaft is older and more mineralized than its ends [60].

Another instance of an advantage of bone’s composite microstructure is in the orientation of lamellae within it. Laminar tissue, where layers form with different angles to the longitudinal axis, aids when tensile stresses deviate from the long bone axis. Oblique fibers provide more resistance to torsional loads than longitudinal or transversely oriented fibers [47]. Therefore, to maximize torsion resistance, the humerus and ulna have a higher degree of laminaarity and higher incidences of oblique collagen fibers than the radius and carpometacarpus [47].

The feather: from nanostructure to mesostructure

Bird feathers are composed exclusively of β -keratin, which is considered a “dead tissue”, and is formed by keratinous cells [61]. The cortex material of the feather can be considered a fiber-reinforced composite with many layers of organization: (1) the sub-nanostructure (~ 3 nm in diameter): crystalline β -keratin filaments embedded in amorphous matrix proteins; (2) the nanostructure (~ 200 nm in diameter): filaments bundle to form macrofibrils which are encompassed by amorphous intermacrofibrillar material; (3) the sub-microstructure (3–5 μm in diameter): macrofibrils organize into fibers; (4) the microstructure (hundreds of microns): fibers form ordered lamellae within the feather shaft cortex (Fig. 10b) [52,61–67]. Discovery of the shaft’s ordered fibers and macrofibrils by Lingham-Soliar et al. [62] sparked a renewed interest in the feather shaft cortex. It has since been shown that the arrangement of the fibrous keratin composite differs between species, possibly based on the flight style of the bird [68–70].

Wang et al. [52] found the California Gull (*Larus californicus*) feather to have a thin outer layer composed of circumferentially wrapped fibers and a thick inner layer of longitudinal fibers within the calamus and the dorsal side of the proximal rachis (Fig. 10c) [52]. This fiber arrangement is commonly used in the design of synthetic composites, and restrains the axial fibers from separating by preventing axial splitting in flexure. Further along the feather, on the dorsal and ventral sides of the distal rachis, there is an increase in longitudinal fibers and decrease of outer circumferential fibers

**FIGURE 9**

Cross sections of the wing feathers of the: (a) Ostrich (*Struthio camelus*), a flightless bird and (b) the American White Pelican (*Pelecanus erythrorhynchos*) a flying bird, where scale bars are 1 mm. Primary feather cross sections at the midpoint of the feather shaft for the (c): (top row, left to right) American White Pelican (*Pelecanus erythrorhynchos*), Andean Condor (*Vultur gryphus*), Razor-Billed Curassow (*Mitu tuberosum*); (bottom row, left to right) Malayan Long-Tailed Parakeet (*Psittacula longicauda*), Marbled Teal (*Marmatonetta angustirostris*), Bartlett's Bleeding Heart Dove (*Gallucolumba crinigera*), Spectacled Eider (*Somateria fischeri*), Crested Guineafowl (*Guttera pucherani*). Fig. 9a adapted from B. Wang et al. (2016) [52].

(Fig. 10d) [52]. Since the elastic modulus is determined by the local fibrous structure, the higher proportion of longitudinally aligned fibers can be correlated to the increase in axial modulus along the length of the feather [52,71]. This increase in elastic modulus along the length of the feather shaft (proximal to distal) has been credited as compensating for the decrease in area moment of inertia along the shaft [30,32,72,73].

Another notable feature of the composite design of the feather shaft is the crossed-fiber structure of the lateral walls of the rachis [52,74]. These fibers are oriented at $\pm 45^\circ$ in this region where dorsal-ventral bending results in primarily shear stresses (Fig. 10d,e). In torsion, the fibers align along the axial stresses, occurring at $\pm 45^\circ$ to the shaft axis. Thus, they improve torsional stiffness with minimum impact on dorsal-ventral bending stiffness [74]. At the same time, lateral deflection can occur without buckling and this stiffness is considerably decreased. Thus, the microstructural composite design of the feather is used to create an efficient material that allows the feather to be strong yet lightweight.

Bioinspired and analogous synthetic designs

Advancements in engineering and design have resulted in solutions similar to those utilized by the avian feather and bone. While some of these solutions are bioinspired, others arose independent to the study of natural systems. Despite recent advances, there is still much room for development of bioinspired materials, structures, and designs using insights from the study of avian feather and bone.

Dense exterior for lightweight torsion resistance

Bird feathers and bones suggest lightweight solutions for torsion resistant structures. Through the process of convergence engineers have developed similar solutions for increasing the torsional stiffness in large container ships, which have significant torsional moments generated by unsymmetrical wave or cargo loading [75–77]. Torsion boxes, or stiffened skins of materials with a lightweight core, are installed in the upper hulls of ships to increase the strength of the ship's exterior in high-risk areas, while maximizing

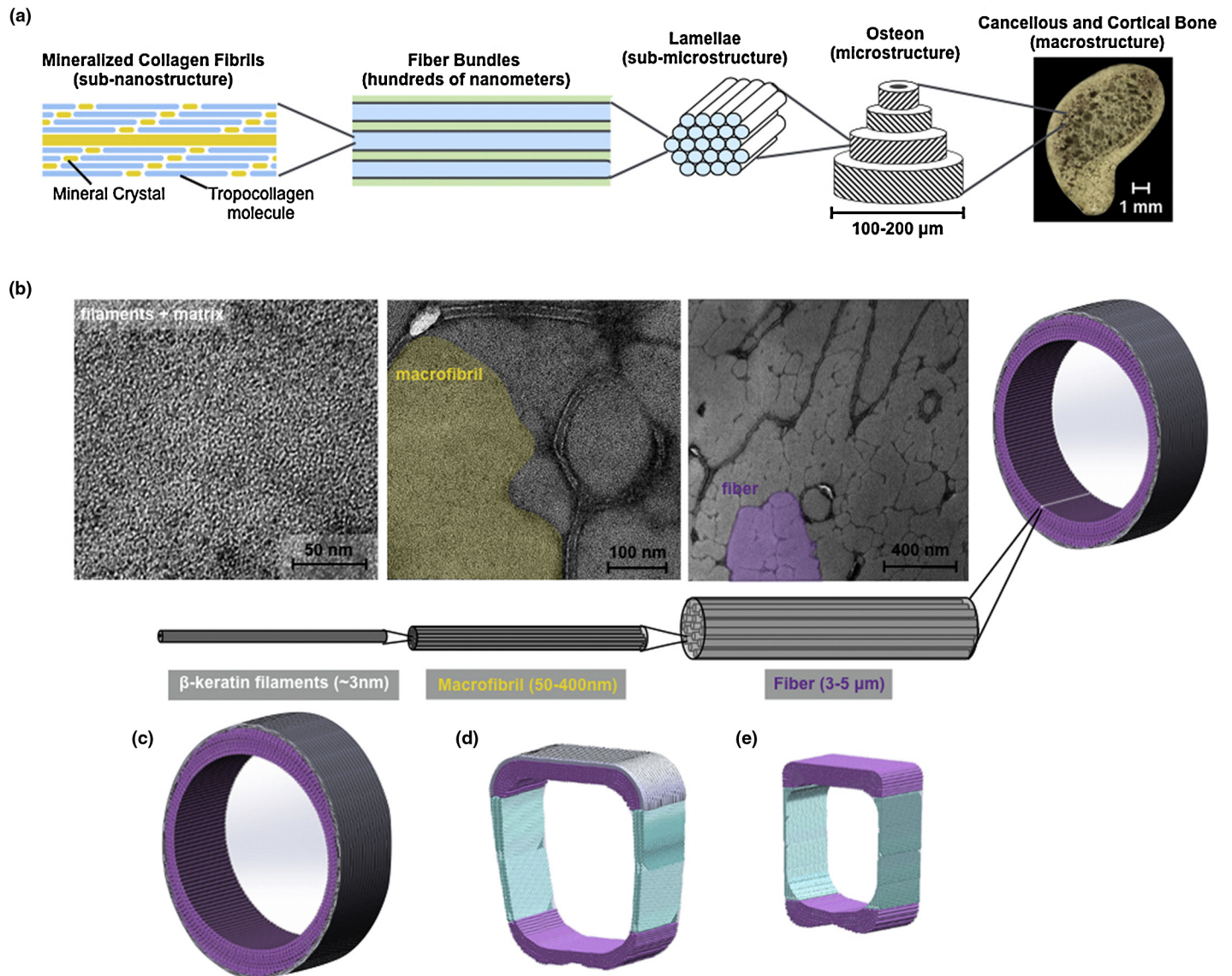


FIGURE 10

The hierarchical structure of bone (a): Tropocollagen molecules and mineral crystals organize to form fiber bundles. These form lamellae that surround an osteon, which form cancellous and cortical bone. The hierarchical structure of the feather shaft cortex (b): β -keratin filaments form macrofibrils and these bundle to form fibers. The orientation of the fibers varies throughout the feather shaft: fibers in the calamus (c) run longitudinally (purple) and circumferentially (gray), within middle and distal rachis (d, e) fibers alternate at angles $\pm 45^\circ$ (green) in the lateral walls. Image (b) from B. Wang, et al. (2016) [109], (c-e) from B. Wang et al. (2016) [52].

space for cargo and minimizing weight [77]. Torsion boxes in ships are analogous to the dense exterior found in torsionally resistant bird bones and feathers.

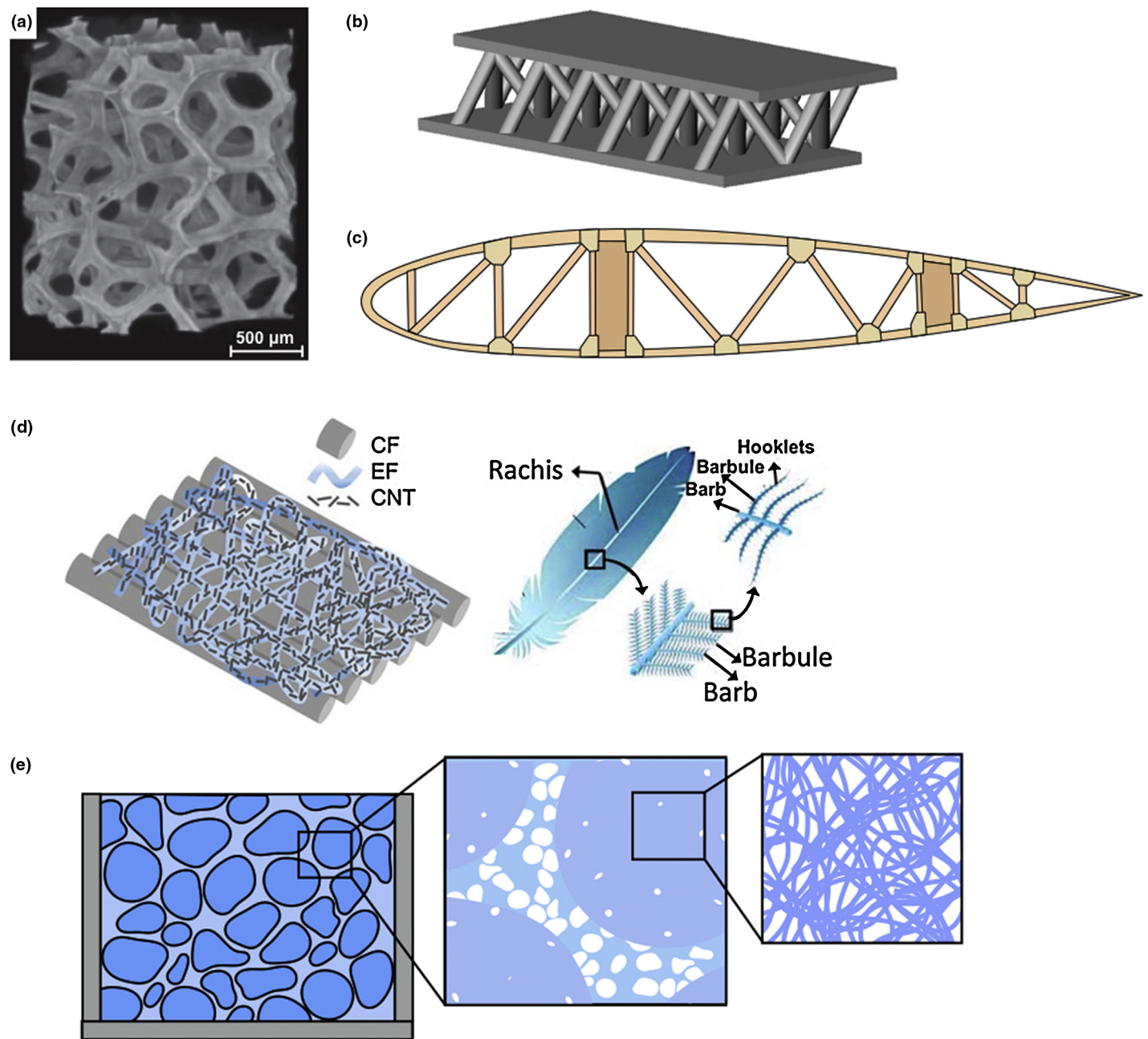
Reinforced internal structures for increased stiffness

Reinforcing struts identified in pneumatic avian bone inspired the fabrication of a nickel metallic foam with criss-crossing “struts” (Fig. 11a) [78]. As in avian bone, these struts provide a lightweight method of maintaining structural integrity. Research has suggested that a structure with a core of angled microstruts (Fig. 11b) is theoretically at least 7 times stiffer than the best open cell foam [79–81]. Although not bioinspired, inclined struts are commonly used to reinforce the ribs of airplane wings (Fig. 11c) [82–84]. These ribs transmit loads from the skin of the wing and stringers to the spars. Similar to the foam-filled feather,

recreational snow skis are designed primarily for a tailored longitudinal stiffness. These skis are composites with faces generally made of aluminum or fiber-reinforced polymer separated by a foam-filled core [26,85–87]. For additional longitudinal reinforcement some skis have reinforcing ridges along their length, similar to the stiffening dorsal ridges of the feather rachis [26,88] shown in Figs. 5c and 9.

Hierarchical composite design

As demonstrated in both the avian feather and bone, hierarchical composites can greatly increase the efficiency and mechanical properties of a structure. Although it is extremely difficult to manufacture materials with the same level of hierarchy as nature, several techniques have been used to fabricate micro- and nano-structured materials including self-assembly, freeze casting

**FIGURE 11**

Engineering has led to similar designs as those found in the avian feather and bone: (a) Nickel metallic foam inspired by the struts in avian bone (taken from X. Jin et al. (2014) [78]), (b) a computer aided design model of diagonal struts in a multifunctional cellular material (taken from A.G. Evans et al. (2001) [79]). The supporting structures in airplane wing ribs (c) have an analogous design and purpose to the struts in avian bone. The hierarchical synthetic composite (d) is inspired by the degrees of hierarchy in the feather (taken from V. Drakonakis et al. (2014) [102]). A foam structure inspired by the fibrous closed-cell structure of the feather's medullary foam (e) would have novel properties.

and electrospinning [89–102]. The latter method was used to create a feather-inspired composite structure with nanofibrous fractal interlayers [102]. In this design, a polymer-carbon nanotube suspension was electrospun onto a carbon fiber bed as an interlayer between lamina. Carbon nanotubes represent the micro- and nano-scale barbules, the electrospun fiber the micro-scale barbs, and the carbon fiber serves as the rachis (Fig. 11d). This composite was shown to have significantly higher mechanical properties than the carbon fiber laminate with no interlayer [102].

Avian wing design

There have been many advances in commercial wing shape; two significant improvements with striking resemblance to the bird wing are winglets and the flexible wing. Winglets are small, roughly vertical surfaces usually located at the wing tips of an aircraft. They are used on aircraft because they can lessen wingtip vortices, reduce drag by about 20%, and allow wings to provide the same amount of lift with a smaller wingspan [103]. Likewise, in many large flying birds, feathers curl upward in flight at wing tips (Fig. 12a) to serve as winglets. A more recent improvement, the

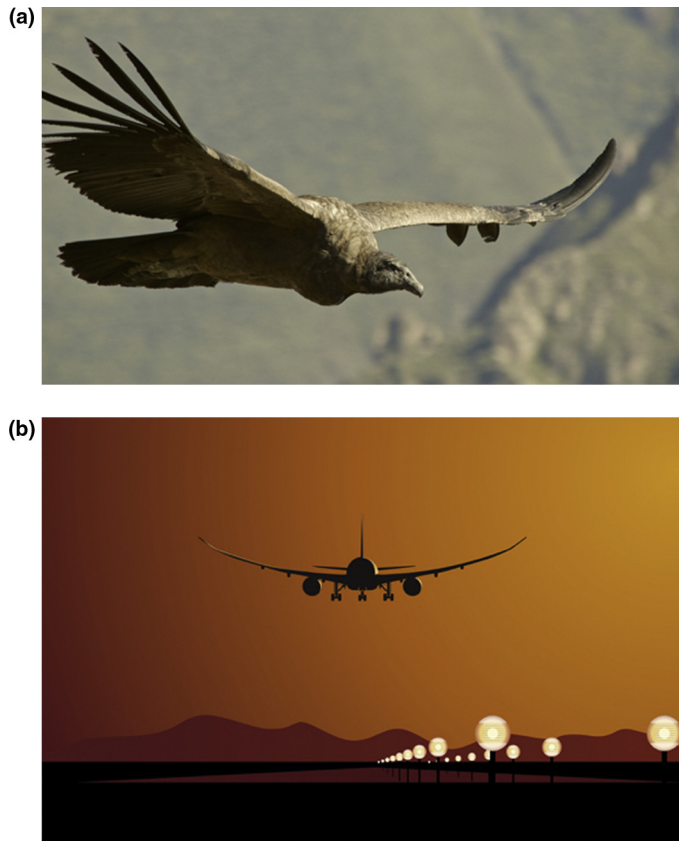


FIGURE 12

Many analogous solutions have been developed through evolution and engineering: (a) The Andean condor's feathers curl upward at its wing tips for more efficient flight. (b) A similar curvature is observed in the flexible wings of a Boeing 787. Images purchased from Dreamstime.

composite wing of the Boeing 787 allows it to flex to be more efficient and dampen turbulence [104,105]. The wing's flexibility is especially apparent in take-off and landing. Similarities between the in-flight wingspan shape of the Andean condor and the Boeing 787 are depicted in Fig. 12a and b, respectively.

Future outlook on avian feather- and bone-inspired designs

The study of avian feather and bone provides fertile opportunity for the development of novel bioinspired structures and materials. For example, the structure of the feather's foam can be mimicked through 3D-printing and/or electrospinning to create a new type of hierarchical foam composed of fibrous closed cells. This "foam within a foam" concept is shown Fig. 11e. This hierarchical foam would result in a novel design that maintains stiffness while decreasing overall weight. Second, by simulating the fiber directionality within the distal rachis, where fibers run longitudinally on the top and bottom and at $\pm 45^\circ$ angles on the sides, a new type of composite I-beam can be created with increased torsional stiffness [106]. Its bending stiffness would be maintained while the $\pm 45^\circ$ fibers would provide additional torsion resistance to expand the functionality of the common I-beam structure. Lastly, a column inspired by the changing shape of the rachis from circular to rectangular provides a structure that is optimized for torsion in one area (circular portion) and for bending stiffness in the other (rectangular portion). A possible use for these structures would be as support columns to create more earthquake-resistant

buildings where both torsional or bending stiffness can be tailored along the length of the column [107].

Conclusions

The features of avian bone and feather discussed in this overview highlight characteristics that enable the bird wing's efficiency. The wing skeleton and flight feathers work together to form an airfoil that supports the bird's mass in flight and undergoes torsional and bending forces while maintaining a minimum weight. Both wing bones and feathers have a thin, dense exterior with reinforcing internal structures, efficiently tailored for the specific bird, and a composite microstructure. The coinciding design principles between these features reveal an apparent evolutionary trend toward structures that efficiently resist bending and torsion.

Wing bones and feathers provide a marvelously complex synergy that not only enables flight but also serves as examples of material-structure specialization for specific functions such as soaring, diving, and flapping. By examining structure-property relationships we reviewed the prominent features, from the nano- to the macroscale, which enable birds to fly. At the nanoscale fibrils of collagen (in bone) and β -keratin (in feathers) arrange to provide fiber bundles that exhibit a high degree of organization leading to superior unidirectional mechanical properties. At the mesoscale these fibrils organize themselves into fibers aligned to resist the specific loading requirements. At the macroscale emergent structural features have evolved to provide an exquisite selection of shape and form which, when combined synergistically with local mesoscale material arrangements, endow birds with ultra-lightweight structures possessing superior resistance to combined bending and torsional loading. In studying the scaling factors in bird feathers, we have uncovered a fascinating fact: while feather shaft length, rachis width and barb length all scale with bird mass, the barbule spacing is approximately the same at 8–16 μm , independent of the size of the bird. We relate this to an optimal size that maintains a balance between vane permeability and interlocking adhesion.

In closing, our overview of bird's wings points at the possibility of framing their design as a combined material and structural optimization problem subject to aerodynamic constraints. While modern research has resulted in some instances of analogous solutions to increase torsional and bending stiffness, there are very few efforts of deliberate bioinspiration of the feather and avian bone. We feel that this is an area rich with opportunity for creating advanced materials and structures. Therefore, we anticipate that with improvements in mathematical and computational tools for *multi-material multi-scale optimization and design*, and experimental tools based on *additive manufacturing*, bioinspiration based on studies reviewed here will be applied to further man-made structures to exhibit the same degree of sophistication and complexity as observed in bird's wings.

Acknowledgements

We would like to thank Alex Hung for creating 3D computer aided design models of the feather vane. We thank Esther Cory and Dr. Robert Sah (UC San Diego) for assistance with μ -CT imaging. We also thank the San Diego Zoo and April Gorow (Research Coordinator), the San Diego Natural History Museum and Phil Unitt (Curator of Birds and Mammals), the Los Angeles Zoo and

Mike Maxcy (Curator of Birds) and Dr. Cathleen Cox (Director of Research), and Raul Aguiar, Rancho La Bellota for providing feather and bone samples to us. We thank Dr. Katya Novitskaya for helpful discussions and Frances Su, Profs. Joanna McKittrick and Michael Tolley for assistance with additive manufacturing. Prof. Michael Porter helped us with the CT scans of several bird bones. Lastly, we thank Isabella Gomez and Israel Rea for image data gathering. This work is part of the AFOSR MURI (AFOSR-FA9550-15-1-0009) and we thank Dr. Hugh DeLong for his support.

References

- [1] J. Clarke, *Science* 340 (2013) 690–692.
- [2] A. Louchart, L. Viriot, *Trends Ecol. Evol.* 26 (2011) 663–673.
- [3] Y. Seki, M. Mackey, M.A. Meyers, *J. Mech. Behav. Biomed. Mater.* 9 (2012) 1–8.
- [4] F.T. Mujres, et al. *PLoS One* 7 (2012).
- [5] A. Wolfson, *A Recent Study in Avian Biology*, University of Illinois Press, Urbana, 1955.
- [6] E.N. Kurochkin, I.A. Bogdanovich, *Biol. Bull.* 35 (2008) 5–17.
- [7] C.J. Pennycuik, *Modelling the Flying Bird*, first ed., Elsevier Inc, Burlington, 2008.
- [8] N.S. Proctor, P.J. Lynch, *Manual of Ornithology: Avian Structure & Function*, first ed., New Haven, Yale UP, 1993.
- [9] F.B. Gill, *Ornithology*, second ed., W.H. Freeman, New York, 1995.
- [10] P.M. O'Connor, L.P.A.M. Claessens, *Nature* 436 (2005) 253–256.
- [11] L. Xing, et al. *Curr. Biol.* 26 (2016) 1–9.
- [12] W. Muller, G. Patone, *J. Exp. Biol.* 201 (1998) 2591–2599.
- [13] J. Dyck, *Zool. Scr.* 14 (1985) 137–154.
- [14] J.J. Videler, in: T.R. Birkhead (Ed.), *Oxford Ornithol. Ser.*, Oxford University Press, Oxford, 2005, pp. 2–7.
- [15] K.E.J. Campbell, E.P. Tonni, *Auk* 100 (1983) 390–403.
- [16] B. Bruderer, et al. *Ibis (Lond. 1859)* 152 (2010) 272–291.
- [17] E. Novitskaya, et al. *Adv. Bioceram. Biotechnol. II* (2014) 47–56.
- [18] J.M.V. Rayner, *Form and Function in Avian Flight*, Plenum Press, New York, 1988.
- [19] C. Pennycuik, *J. Exp. Biol.* 46 (1967) 219–233.
- [20] I.H. Abbott, A.E. von Doenhoff, *Theory of Wing Sections*, Dover Publications, New York, 1959.
- [21] S.M. Swartz, M.B. Bennett, D.R. Carrier, *Nature* 356 (1992) 133–135.
- [22] F.P. Beer, et al., *Mechanics of Materials*, fifth ed., McGraw-Hill, New York, 2009.
- [23] E.P. Popov, *Engineering Mechanics of Solids*, second ed., Prentice Hall, Upper Saddle River, 1998.
- [24] R. Ennos, *Solid Biomechanics*, Princeton University Press, Princeton, 2012.
- [25] E.R. Dumont, *Proc. Biol. Sci.* 277 (2010) 2193–2198.
- [26] L.J. Gibson, M.F. Ashby, *Cellular Solids: Structure & Properties*, second ed., Cambridge University Press, Cambridge, 1997.
- [27] J. Cubo, A. Casinos, *Zool. J. Linn. Soc.* 130 (2000) 499–510.
- [28] J.D. Currey, R.McN. Alexander, *J. Zool. Lond.* 206 (1985) 453–468.
- [29] M.A. Meyers, et al. *Prog. Mater. Sci.* 53 (2008) 1–206.
- [30] R.H.C. Bonser, P.P. Purslow, *J. Exp. Biol.* 198 (1995) 1029–1033.
- [31] I.M. Weiss, H.O.K. Kirchner, *J. Exp. Zool. A: Ecol. Genet. Physiol.* 313 (2010) 690–703.
- [32] T. Bachmann, et al. *J. Exp. Biol.* 215 (2012) 405–415.
- [33] D.G. Crenshaw, *Symp. Soc. Exp. Biol.* 43 (1980) 485–486.
- [34] R.H.C. Bonser, *J. Zool.* 239 (1996) 477–484.
- [35] P.P. Purslow, J.F.V. Vincent, *J. Exp. Biol.* 72 (1978) 251–260.
- [36] E. Novitskaya, et al. *Unpublished results* (2017).
- [37] W.R. Corning, A.A. Biewener, *J. Exp. Biol.* 201 (1998) 3057–3065.
- [38] M. Olmos, A. Casinos, J. Cubo, *Ann. Nat. Sci. Zool. Anim. Biol.* 17 (1996) 39–49.
- [39] R.E. Brown, A.C. Cogley, *J. Exp. Zool.* 276 (1996) 112–124.
- [40] H. Tennekkes, *The Simple Science of Flight: From Insects to Jumbo Jets*, second ed., MIT Press, Cambridge, MA, 2009.
- [41] T.N. Sullivan, M.A. Meyers, *Unpublished* (2017).
- [42] S.E. Worcester, *J. Zool.* 239 (1996) 609–624.
- [43] X. Wang, et al. *J. Evol. Biol.* 25 (2012) 547–555.
- [44] A. Azuma, *The Biokinetics of Flying and Swimming*, second ed., American Institute of Aeronautics and Astronautics, Inc, Reston, VA, 2006.
- [45] P. Gopalakrishnan, D.K. Tafti, *AIAA J.* 48 (2010) 865–877.
- [46] A.M. Mountcastle, S.A. Combes, *Proc. Biol. Sci.* 280 (2013) 20130531.
- [47] E. De Margerie, et al. *Anat. Rec. A: Discov. Mol. Cell. Evol. Biol.* 282 (2005) 49–66.
- [48] J. Kiang, *Avian Wing Bones*, (M.Sc. Thesis), University of California, San Diego, 2013.
- [49] J. Cubo, L. Menten, A. Casinos, *Ann. Des. Sci. Nat. Zool. Biol. Anim.* 20 (1999) 153–159.
- [50] K.P. Dial, *Auk* 109 (1992) 874–885.
- [51] Z.Q. Liu, et al. *Acta Biomater.* 17 (2015) 137–151.
- [52] B. Wang, M.A. Meyers, *Adv. Sci.* 4 (2017), <http://dx.doi.org/10.1002/adv.201600360>.
- [53] H.D. Espinosa, et al. *Prog. Mater. Sci.* 54 (2009) 1059–1100.
- [54] J.Y. Rho, L. Kuhn-Spearing, P. Zioupos, *Med. Eng. Phys.* 20 (1998) 92–102.
- [55] N. Reznikov, R. Shahar, S. Weiner, *Acta Biomater.* 10 (2014) 3815–3826.
- [56] S. Weiner, W. Traub, *FASEB J.* 6 (1992) 879–885.
- [57] H.D. Barth, et al. *Biomaterials* 32 (2011) 8892–8904.
- [58] P. Fratzl, et al. *J. Mater. Chem.* 14 (2004) 2115–2123.
- [59] K.J. Bundy, *Composite Material Models for Bone*, CRC Press, Boca Raton, FL, 1989.
- [60] R.H. Bonser, *J. Exp. Biol.* 198 (1995) 209–212.
- [61] B. Wang, et al. *Prog. Mater. Sci.* 76 (2016) 229–318.
- [62] T. Lingham-Soliar, R.H.C. Bonser, J. Wesley-Smith, *Proc. R. Soc. Biol. Sci.* 277 (2010) 1161–1168.
- [63] J. McMurry, R. Fay, *Chemistry: Biochemistry*, Pearson Prentice Hall, 2003.
- [64] R.D.B. Fraser, T.P. MacRae, G.E. Rogers, *Keratins: Their Composition, Structure and Biosynthesis*, 1972.
- [65] R.D.B. Fraser, D.A.D. Parry, *J. Struct. Biol.* 176 (2011) 340–349.
- [66] J. McKittrick, et al. *JOM* 64 (2012) 449–468.
- [67] T. Lingham-Soliar, N. Murugan, *PLoS One* 8 (2013).
- [68] C.M. Laurent, C. Palmer, R.P. Boardman, G. Dyke, R.B. Cook, *J. R. Soc. Interface* 11 (2014).
- [69] B. Bussón, P. Engström, J. Doucet, *J. Synchrotron Radiat.* 6 (1999) 1021–1030.
- [70] C.M. Laurent, et al. *J. R. Soc. Interface* 11 (2014) 20140961.
- [71] G.J. Cameron, T.J. Wess, R.H.C. Bonser, *J. Struct. Biol.* 143 (2003) 118–123.
- [72] T. Bachmann, et al. *Front. Zool.* 4 (2007) 23.
- [73] G.D. Macleod, *J. Exp. Biol.* 87 (1980) 65–71.
- [74] T. Lingham-Soliar, *J. Ornithol.* 155 (2013) 323–336.
- [75] J.K. Paik, et al., *Ultimate Strength of Ship Hulls under Torsion*, 2001.
- [76] K. Iijima, et al. *Mar. Struct.* 17 (2004) 355–384.
- [77] E. Alfred Mohammed, et al. *Mar. Struct.* 46 (2016) 78–101.
- [78] X. Jin, et al. *Adv. Funct. Mater.* 24 (2014) 2721–2726.
- [79] A.G. Evans, et al. *Prog. Mater. Sci.* 46 (2001) 309–327.
- [80] M.F. Ashby, et al., *Metal Foams A Design Guide*, Elsevier, 2000.
- [81] B. Budiansky, *Int. J. Solids Struct.* 36 (1999) 3677–3708.
- [82] Federal Aviation Administration, *Aviat. Maint. Tech. Handb. – Airframe* (2012) 48.
- [83] L. Krog, et al. 10th AIAA/ISSMO Multidiscip. Anal. Optim. Conf., American Institute of Aeronautics and Astronautics, Albany, NY, (2004), pp. 1–16.
- [84] G.D. Swanson, Z. Gurdal, J.H. Starnes, *J. Aircr.* 27 (1990) 1011–1020.
- [85] K.D. Schmidt, M.A. Robinson, *Fiber Glass Ski with Channel Construction*, 3503621, 1970.
- [86] J.G. Howe, *Ski Construction*, 5820154, 1998.
- [87] H.M. Anderson, *Laminated Ski Having a Foam Filled Honeycomb Core*, 3276784, 1966.
- [88] W.H. Vinton, *Ski*, 2277281, 1942.
- [89] C. Sanchez, H. Arribart, M.M.G. Guille, *Nat. Mater.* 4 (2005) 277–288.
- [90] M. Li, H. Schnablegger, S. Mann, *Nature* 402 (1999) 393–395.
- [91] C.M. Niemeyer, et al. *Biochem. Biophys. Res. Commun.* 311 (2003) 995–999.
- [92] D. Iacopino, et al. *Nanotechnology* 14 (2003) 447–452.
- [93] B.W. Shenton, S.A. Davis, S. Mann, *Adv. Mater.* 11 (1999) 449–452.
- [94] S. Deville, et al. *Science* 311 (2006) 515–518.
- [95] S. Sadeghpour, et al. *Ceram. Int.* 40 (2014) 16107–16114.
- [96] M. Hafezi, et al. *J. Mater. Sci.* 49 (2014) 1297–1305.
- [97] L. Jing, et al. *Ceram. Int.* 36 (2010) 2499–2503.
- [98] M. Bognitzki, et al. *Adv. Mater.* 13 (2001) 70–72.
- [99] R. Ramaseshan, et al. *J. Appl. Phys.* 102 (2007).
- [100] M.P. Prabhakaran, J. Venugopal, S. Ramakrishna, *Acta Biomater.* 5 (2009) 2884–2893.
- [101] R. Ostermann, et al. *Nano Lett.* 6 (2006) 1297–1302.
- [102] V.M. Drakonakis, et al. *Polym. Compos.* (2014).
- [103] R.T. Whitcomb, *A Design Approach and Selected Wind-Tunnel Results at High Subsonic Speeds for Wing-Tip Mounted Winglets*, 1976.
- [104] Boeing (2017).
- [105] J. Paur, *Wired*, 2010.
- [106] A. Ghobarah, M.N. Ghorbel, S.E. Chidiac, *J. Compos. Constr.* 6 (2002) 257–263.
- [107] C. Arnold, *Des. Earthquakes, A Man. Archit.*, Federal Emergency Management Agency, 2006.
- [108] T.N. Sullivan, et al. *Acta Biomater.* 41 (2016) 27–39.
- [109] B. Wang, M.A. Meyers, *Acta Biomater.* 48 (2017) 270–288.